Available online at www.sciencedirect.com
SCIENCE DIRECT®
Journal of Computational Physics 193 (2004) 544–562
JOURNAL OF COMPUTATIONAL PHYSICS
www.elsevier.com/locate/jcp

A linear iterative scheme for the fast solution of the radiative heat transfer equations for glass ☆

Guido Thömmes

Department of Mathematics, Technical University of Darmstadt, Weidenweg 14, 52074 Aachen, Darmstadt 64289, Germany

Received 24 March 2003; received in revised form 5 August 2003; accepted 5 August 2003

Abstract

In this paper, a linear, iterative solver for the radiative heat transfer (RHT) equations appearing in the simulation of glass cooling is studied. The solver becomes slow if the regime is optically thick, i.e., if absorption and scattering of radiation are strong. We propose a preconditioning technique for the RHT equations analogous to DSA preconditioning for the radiative transport equation using the P_1 approximation corresponding to the system investigated. Numerical investigations demonstrate the feasibility and performance of the approach.

1. Introduction

The temperature evolution in a glass slab can be mathematically modeled by the radiative heat transfer (RHT) equations, i.e., a coupled system of a heat equation and a radiative transfer equation [8,14,18,19]. This reflects the underlying physics of glass cooling where heat conduction and radiation are the dominant processes for energy transfer. The coupling of the two equations is done by energy exchange terms between the radiation of the hot glass and the radiation field. Fast solvers are needed because simulations are computationally costly, primarily due to the fact that the radiation has to be calculated not only for each position but also for each direction. Efficient simulation of radiative processes, therefore, is still a challenging task and an area of active research with a wide range of applications not only in glass cooling but also in the design of gas turbines, for example.

In this paper, we consider a simple Richardson iteration for a semi-discretized RHT system with discretized time and continuous space variable, and for a fully discretized system. When this iteration is used, convergence becomes slow in the optically thick regime such that an acceleration technique

☆ This work has been supported by DFG Grant KL 1105/7 and by SFB 568.
E-mail address: guido_thoemmes@web.de (G. Thömmes).

0021-9991/$ - see front matter © 2003 Elsevier B.V. All rights reserved.
doi:10.1016/j.jcp.2003.08.024

has to be employed. We propose an iterative scheme that uses the P_1 approximation to the RHT equations as a preconditioner. The procedure is motivated by the ideas used in the construction of the fast DSA solver, which is a highly effective preconditioning technique for the transport equation and which has been intensively studied in the realm of neutron transport theory [1,9,12]. In fact, it extends the method applied to the stationary transport equation to the case of the stationary RHT equations. Moreover, the method we propose uses DSA as a basic building block for solving the radiation equation. We also refer, e.g., to [3,15] for other applications of the DSA method to thermal radiative transfer problems.

We consider the following system of non-dimensional RHT equations in one-dimensional *slab geometry* on the unit interval $x \in [0,1]$ in space and for all times $t > 0$

$$\varepsilon^2 \frac{\partial T}{\partial t} = \varepsilon^2 \partial_x (k \partial_x T) + \langle \kappa (I - B) \rangle, \tag{1.1a}$$

$$\forall \mu \in [-1,1]: \quad \varepsilon \mu \partial_x I + \sigma_s I = \frac{1}{4\pi} \langle \sigma_s I \rangle + \kappa (B - I), \tag{1.1b}$$

where $T = T(x,t)$ denotes the temperature and $I = I(x,t,\mu)$ represents the (direction-dependent) radiative intensity. The brackets indicate integration over all directions, i.e., in 1D we have $\langle I \rangle = 2\pi \int_{-1}^{+1} I(\mu)\,\mathrm{d}\mu$ [10]. Eqs. (1.1a) and (1.1b) contain the heat conductivity k, the scattering and the absorption cross-sections σ_s, κ, respectively, and the non-dimensional parameter ε. They are assumed to be constants. The total spectral intensity B for a Planckian in glass is given by Stefan's Law according to

$$B(T) = n^2 \frac{\sigma}{\pi} T^4$$

with the refraction index n of glass and the Stefan–Boltzmann constant σ. On the boundary, for $x = 0$ or $x = 1$, the ingoing radiation is prescribed by transparent boundary conditions

$$\forall \mu > 0: \quad I(\mu,0) = I_b(\mu,0) \quad \text{and} \quad \forall \mu < 0: \quad I(\mu,1) = I_b(\mu,1), \tag{1.1c}$$

while the temperature is assumed to obey Dirichlet boundary conditions

$$T(0) = T_l, \quad T(1) = T_r. \tag{1.1d}$$

Boundary values are assumed to be constant with respect to time t. At initial time $t = 0$ the temperature is $T(x,0) = T_0(x)$.

2. Linear, iterative scheme for RHT equations

We begin by making the following observation in order to obtain a linear semi-discretized system of equations that can be solved using a linear iterative method. Using $B \sim T^4$ from Stefan's Law for Planck's radiation as an independent variable instead of the temperature T [7], Eq. (1.1a) reads

$$\varepsilon^2 \frac{\partial B}{\partial t} = \varepsilon^2 (B') \partial_x \left(\frac{k}{(B')} \partial_x B \right) + (B') \langle \kappa (I - B) \rangle, \tag{2.1}$$

with $B' = \mathrm{d}B/\mathrm{d}T$. If we discretize time at this point in the following semi-implicit way then

$$\varepsilon^2 \frac{B^{(n+1)} - B^{(n)}}{\Delta t} = \varepsilon^2 (B')^{(n)} \partial_x \left(\frac{k}{(B')^{(n)}} \partial_x B^{(n+1)} \right) + (B')^{(n)} \langle \kappa (I^{(n+1)} - B^{(n+1)}) \rangle$$

$$\forall \mu \in [-1,1]: \ \varepsilon \mu \partial_x I^{(n+1)} + \sigma_s I^{(n+1)} = \frac{1}{4\pi} \langle \sigma_s I^{(n+1)} \rangle + \kappa (B^{(n+1)} - I^{(n+1)}).$$

At each time step a linear system has to be solved:

$$\left[\varepsilon^2 + \Delta t (B')^{(n)} 4\pi\kappa - \varepsilon^2 \Delta t (B')^{(n)} \partial_x \left(\frac{k}{(B')^{(n)}} \partial_x (\cdot) \right) \right] B^{(n+1)} - \Delta t (B')^{(n)} \kappa \langle I^{(n+1)} \rangle = \varepsilon^2 B^{(n)}, \tag{2.2a}$$

$$-\kappa B^{(n+1)} + \left[\varepsilon \mu \partial (\cdot) + \sigma_s + \kappa - \frac{\sigma_s}{4\pi} \langle \cdot \rangle \right] I^{(n+1)} = 0, \tag{2.2b}$$

or more formally written in operator–matrix notation

$$\begin{bmatrix} A_{11} & A_{12} \\ A_{21} & A_{22} \end{bmatrix} \begin{bmatrix} B^{(n+1)} \\ I^{(n+1)} \end{bmatrix} = \begin{bmatrix} b_T \\ b_I \end{bmatrix} = \begin{bmatrix} \varepsilon^2 B^{(n)} \\ 0 \end{bmatrix}. \tag{2.2c}$$

The elliptic operator A_{11} and the transport operator A_{22} are well known and can be efficiently solved using standard methods. For A_{22} the method of choice in the 1D case is the *DSA iteration*, which is highly efficient for large class of problems even in the optically thick regime [12]. This observation and the form of (2.2c) suggest an iterative approach of block type for solving the semi-discretized system above. For our investigation we took Jacobi and block Gauss–Seidel into account. To keep the presentation short we focus in the sequel on a Gauss–Seidel iteration using the upper triangular part of the block matrix. This is no restriction because similar results can be obtained in the other cases using the same procedure (see Appendices A and B).

Using the upper triangular matrix in (2.2c), the linear iteration is given by

$$\text{for } k \geqslant 1: \quad \begin{bmatrix} A_{11} & A_{12} \\ 0 & A_{22} \end{bmatrix} \begin{bmatrix} B_{k+1} \\ I_{k+1} \end{bmatrix} = \begin{bmatrix} \varepsilon^2 B^{(n)} \\ -A_{21} B_k \end{bmatrix}. \tag{2.3}$$

The initial iterates $B_0 = B^{(n)}$ and $I_0 = I^{(n)}$ are chosen to start the iteration. Numerical experiments in the area of glass cooling applications reveal that convergence becomes unacceptingly slow in the optically thick regime, i.e., if ε is small. To assess this behaviour we investigate the reduction of the error using a von Neumann analysis. In order to do so, an infinite, homogeneous-space medium has to be assumed and, furthermore, $(B')^{(n)}(T)$, has to be constant with respect to x. These are strong restrictions, but a similar von Neumann analysis has been carried out for source iteration and DSA and gives important insight into these algorithms [1]. The results obtained there remain largely valid in many other cases, e.g., for inhomogeneous media on finite domains. Therefore, the author believes that the following investigations are valid in a wider range of cases as well.

Introducing the error of the Planckian and of the radiative intensity

$$b_k = B^* - B_k \quad \text{with } B^* = B^{(n+1)},$$
$$i_k = I^* - I_k, \quad I^* = I^{(n+1),}$$

where B^* and I^* are the true solutions of the system (2.2c), the errors fulfill

$$\text{for } k \geqslant 0: \quad \begin{bmatrix} A_{11} & A_{12} \\ 0 & A_{22} \end{bmatrix} \begin{bmatrix} b_{k+1} \\ i_{k+1} \end{bmatrix} = \begin{bmatrix} 0 \\ -A_{21} b_k \end{bmatrix}, \tag{2.4a}$$

or more explicitly

$$\left[\varepsilon^2 + \Delta t (B')^{(n)} 4\pi\kappa - \varepsilon^2 \Delta t (B')^{(n)} \partial_x \left(\frac{k}{(B')^{(n)}} \partial_x (\cdot) \right) \right] b_{k+1} - \Delta t (B')^{(n)} \kappa \langle i_{k+1} \rangle = 0, \tag{2.4b}$$

$$\left[\varepsilon\mu \partial(\cdot) + \sigma_s + \kappa - \frac{\sigma_s}{4\pi} \langle \cdot \rangle \right] i_{k+1} = \kappa b_k. \tag{2.4c}$$

An ansatz for the errors in terms of Fourier modes w.r.t the space variable x ($\bar{\jmath}^2 = -1$) is made

$$b_k(x) = \hat{b}_k(\xi)\, \mathrm{e}^{\bar{\jmath}\xi x}, \quad i_k(x,\mu) = \hat{\imath}_k(\xi,\mu)\, \mathrm{e}^{\bar{\jmath}\xi x}$$

and inserted into (2.4b) and (2.4c). Then

$$\left[\varepsilon^2 + \Delta t (B')^{(n)} 4\pi\kappa - \varepsilon^2 k \Delta t (\bar{\jmath}\xi)^2 \right] \hat{b}_{k+1} - \Delta t (B')^{(n)} \kappa \langle \hat{\imath}_{k+1} \rangle = 0, \tag{2.5a}$$

$$\left[\varepsilon\mu (\bar{\jmath}\xi) + \sigma_s + \kappa - \frac{\sigma_s}{4\pi} \langle \cdot \rangle \right] \hat{\imath}_{k+1} = \kappa \hat{b}_k. \tag{2.5b}$$

Defining constants

$$C_1 = \Delta t (B')^{(n)} 4\pi\kappa, \quad C_2 = k\Delta t \quad \text{and} \quad \chi = \varepsilon^2 + C_1 + C_2 \varepsilon^2 \xi^2,$$

the first equation may be shortly written

$$\hat{b}_{k+1} = \frac{C_1}{4\pi\chi} \langle \hat{\imath}_{k+1} \rangle.$$

Moreover, Eq. (2.5b) allows for the computation of the total radiation

$$\langle \hat{\imath}_{k+1} \rangle = \left(\frac{\sigma_s}{4\pi} \langle \hat{\imath}_{k+1} \rangle + \kappa \hat{b}_k \right) 2\pi \int_{-1}^{+1} \frac{\mathrm{d}\mu}{\sigma_t + \kappa + \bar{\jmath}\varepsilon\xi\mu} = \left(\frac{\sigma_s}{\kappa + \sigma_s} \langle \hat{\imath}_{k+1} \rangle + \frac{\kappa}{\kappa + \sigma_s} 4\pi \hat{b}_k \right) \frac{1}{2} \int_{-1}^{+1} \frac{\mathrm{d}\mu}{1 + \bar{\jmath} \frac{\varepsilon\xi\mu}{\kappa + \sigma_s}}.$$

The integral on the right can be written

$$S = \frac{1}{2} \int_{-1}^{+1} \frac{\mathrm{d}\mu}{1 + \bar{\jmath} \frac{\varepsilon\xi\mu}{\kappa + \sigma_s}} = \frac{1}{2} \int_{-1}^{+1} \frac{\mathrm{d}\mu}{1 + \left(\frac{\varepsilon\xi\mu}{\kappa + \sigma_s} \right)^2} = \frac{\sigma_s + \kappa}{\varepsilon\xi} \arctan \frac{\varepsilon\xi}{\sigma_s + \kappa}.$$

When the following variables are defined

$$\Sigma = \frac{\varepsilon\xi}{\sigma_s + \kappa}, \quad \omega_0 = \frac{\frac{\kappa}{\sigma_s + \kappa} \frac{\arctan \Sigma}{\Sigma}}{1 - \frac{\sigma_s}{\sigma_s + \kappa} \frac{\arctan \Sigma}{\Sigma}} \quad \text{and} \quad \omega = \frac{C_1}{\chi} \omega_0,$$

the expression for the intensity's new Fourier mode is

$$\langle \hat{\imath}_{k+1} \rangle = 4\pi\omega_0 \hat{b}_{k+1} = \frac{C_1}{\chi} \omega_0 \langle \hat{\imath}_k \rangle = \omega \langle \hat{\imath}_k \rangle.$$

This result may be summarized by writing the 2×2 system

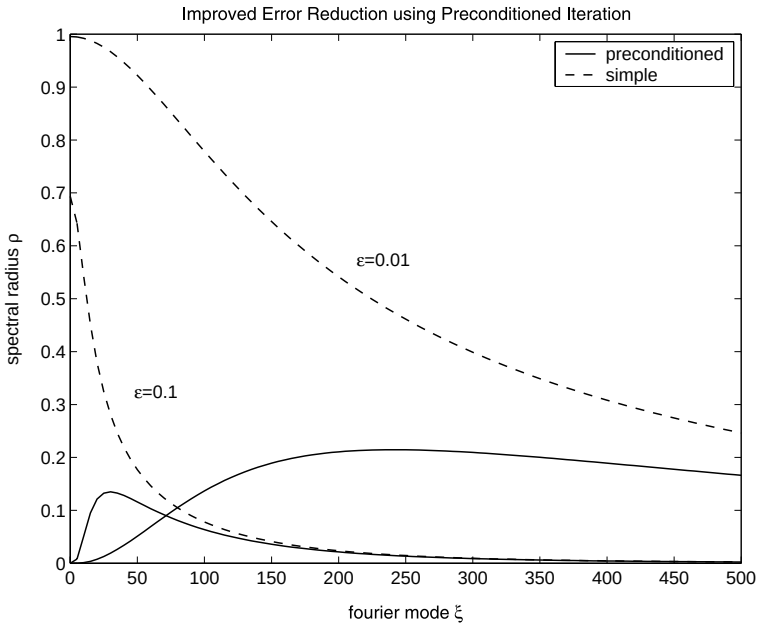

Fig. 1. Spectral radius for the simple and the preconditioned iterations as a function of ξ for two parameter values $\varepsilon = 0.1$ and $\varepsilon = 0.01$, respectively ($\sigma_s = 0$).

$$\text{for } k \geqslant 0: \quad \begin{bmatrix} \hat{b}_{k+1} \\ \langle \hat{\imath}_{k+1} \rangle \end{bmatrix} = \begin{bmatrix} \omega & 0 \\ 4\pi\omega_0 & 0 \end{bmatrix} \begin{bmatrix} \hat{b}_k \\ \langle \hat{\imath}_k \rangle \end{bmatrix} \tag{2.6}$$

for the recursive evolution of the Fourier modes. It can be seen that the spectral radius, i.e., the largest eigenvalue of the matrix is given by

$$\rho_0 \equiv \rho_0(\varepsilon, \xi) = |\omega(\varepsilon, \xi)| = \frac{C_1}{\varepsilon^2 + C_1 + C_2\varepsilon^2\xi^2} \frac{\frac{\kappa}{\sigma_s+\kappa} \frac{\arctan \Sigma}{\Sigma}}{1 - \frac{\sigma_s}{\sigma_s+\kappa} \frac{\arctan \Sigma}{\Sigma}}. \tag{2.7}$$

Making use of the relations

$$0 < \frac{\arctan \Sigma}{\Sigma} < 1, \quad \lim_{\Sigma \to 0} \frac{\arctan \Sigma}{\Sigma} = 1, \quad \lim_{\Sigma \to \pm\infty} \frac{\arctan \Sigma}{\Sigma} = 0,$$

for $\Sigma \neq 0$, we find

$$\rho_0(\varepsilon, \xi) < 1 \quad \text{and} \quad \lim_{\xi \to 0} \rho_0(\varepsilon, \xi) = \frac{C_1}{\varepsilon^2 + C_1}, \quad \lim_{(\varepsilon,\xi) \to (0,0)} \rho_0(\varepsilon, \xi) = 1.$$

This implies, first of all, that the iteration converges. Nevertheless, convergence becomes slow when ε is small, i.e., in the optically thick regime. Convergence becomes also slow if ξ is small, i.e., for the long-wavelength contributions of the error varying on large space scales. It may be noted, however, that short wavelengths corresponding to $\xi \gg 1$ are always damped fast. Fig. 1 illustrates this behaviour.

3. Acceleration using the P_1 approximation

The previous section showed that the difficulty is that the convergence rates approach 1 when ξ becomes small such that the resulting convergence is slow. To remedy the shortcomings of the simple iterative

method described above a preconditioning technique is applied. The procedure is analogous to the DSA preconditioning developed for the radiative transfer equation in 1D, where the approach was successfully introduced. An approximation to the error is added as a correction to the current iterate. If the error could be computed exactly this would immediately lead to the solution. However, since this would amount to solving a similar RHT system of equations as before, such an approach is not feasible and we resort to approximating the system for the errors by the corresponding P_1 approximation. It turns out that this procedure improves the convergence rates in the desired way.

Recall that the P_1 approximation for a radiative transport equation in the form

$$\forall \mu \in [-1,1]: \quad \varepsilon \mu \partial_x I + (\sigma_s + \kappa) I = \frac{1}{4\pi} \langle \sigma_s I \rangle + \kappa B$$

is given by

$$-\frac{\varepsilon^2}{3(\sigma_s + \kappa)} \Delta \varphi + \kappa \varphi = 4\pi \kappa B \quad \text{in } V$$

$$\text{with Robin b.c.} \quad \varphi + \frac{2\varepsilon}{3(\sigma_s + \kappa)} n \cdot \nabla \varphi = 4 I_1 \quad \text{on } \partial V,$$

where $\varphi = \langle I \rangle$ is the total radiative energy and an approximation to the intensity is recovered by $I \approx \frac{1}{4\pi}(\varphi - 3\mu \partial_x \varphi)$ [13,16,17].

We propose the following preconditioned scheme. In a first step, solve.

$$\left[\varepsilon^2 + \Delta t (B')^{(n)} 4\pi\kappa - \varepsilon^2 \Delta t (B')^{(n)} \partial_x \left(\frac{k}{(B')^{(n)}} \partial_x (\cdot) \right) \right] B_{k+\frac{1}{2}} - \Delta t (B')^{(n)} \kappa \langle I_{k+\frac{1}{2}} \rangle = \varepsilon^2 B^{(n)}, \tag{3.1a}$$

$$-\kappa B_k + \left[\varepsilon \mu \partial (\cdot) + \sigma_s + \kappa - \frac{\sigma_s}{4\pi} \langle \cdot \rangle \right] I_{k+\frac{1}{2}} = 0. \tag{3.1b}$$

Then, the errors $b_{k+\frac{1}{2}}$ and $i_{k+\frac{1}{2}}$ fulfill the *error equations*

$$\left[\varepsilon^2 + \Delta t (B')^{(n)} 4\pi\kappa - \varepsilon^2 \Delta t (B')^{(n)} \partial_x \left(\frac{k}{(B')^{(n)}} \partial_x (\cdot) \right) \right] b_{k+\frac{1}{2}} - \Delta t (B')^{(n)} \kappa \langle i_{k+\frac{1}{2}} \rangle = 0,$$

$$\left[\varepsilon \mu \partial (\cdot) + \sigma_s + \kappa - \frac{\sigma_s}{4\pi} \langle \cdot \rangle \right] i_{k+\frac{1}{2}} = \kappa b_{k+\frac{1}{2}} + \kappa (B_{k+\frac{1}{2}} - B_k),$$

which are approximated by replacing the transfer equation by its corresponding P_1 equation as indicated above. The approximation may be written in the form

$$\left[\varepsilon^2 - \varepsilon^2 \Delta t (B')^{(n)} \partial_x \left(\frac{k}{(B')^{(n)}} \partial_x (\cdot) \right) \right] \theta_{k+\frac{1}{2}} - \frac{\varepsilon^2 \Delta t (B')^{(n)}}{3(\sigma_s + \kappa)} \Delta \varphi_{k+\frac{1}{2}} = \Delta t (B')^{(n)} 4\pi\kappa (B_{k+\frac{1}{2}} - B_k), \tag{3.2a}$$

$$-4\pi\kappa \theta_{k+\frac{1}{2}} + \left[-\frac{\varepsilon^2}{3(\sigma_s + \kappa)} \partial_x^2 (\cdot) + \kappa \right] \varphi_{k+\frac{1}{2}} = 4\pi\kappa (B_{k+\frac{1}{2}} - B_k). \tag{3.2b}$$

Note that (3.2b) is inserted in the heat equation resulting in the second Laplacian in (3.2a). Eqs. (3.2a) and (3.2b) represent the approximate system that is solved in order to calculate corrections $\theta_{k+\frac{1}{2}}$, $\varphi_{k+\frac{1}{2}}$ for $B_{k+\frac{1}{2}}$ and $I_{k+\frac{1}{2}}$, respectively. Finally, an update is made to complete a full step of the preconditioned iteration:

$$B_{k+1} = B_{k+\frac{1}{2}} + \theta_{k+\frac{1}{2}},$$
$$\langle I_{k+1}\rangle = \langle I_{k+\frac{1}{2}}\rangle + \varphi_{k+\frac{1}{2}}. \tag{3.3}$$

Again, some insight into the behaviour of the new scheme can be gained by performing a von Neumann analysis. As shown by (2.6) in Section 2, the amplitude of a Fourier mode of the error in the first step is propagated according to

$$\text{for } k \geqslant 0: \quad \begin{bmatrix} \hat{b}_{k+\frac{1}{2}} \\ \langle \hat{\imath}_{k+\frac{1}{2}}\rangle \end{bmatrix} = \begin{bmatrix} \omega & 0 \\ 4\pi\omega_0 & 0 \end{bmatrix} \begin{bmatrix} \hat{b}_k \\ \langle \hat{\imath}_k\rangle \end{bmatrix}. \tag{3.4}$$

For the second step, a Fourier ansatz for $\theta_{k+\frac{1}{2}}$ and $\varphi_{k+\frac{1}{2}}$

$$\theta_{k+\frac{1}{2}}(x) = \hat{\theta}_{k+\frac{1}{2}}(\xi)\,\mathrm{e}^{\bar{\jmath}\xi x}, \quad \varphi_{k+\frac{1}{2}}(x) = \hat{\varphi}_{k+\frac{1}{2}}(\xi)\,\mathrm{e}^{\bar{\jmath}\xi x}$$

is introduced into (3.2a) and (3.2b) and we obtain

$$\left[\varepsilon^2 - \Delta t k \varepsilon^2 (\bar{\jmath}\xi)^2\right]\hat{\theta}_{k+\frac{1}{2}} - \frac{\varepsilon^2 \Delta t (B')^{(n)}}{3(\sigma_s+\kappa)}(\bar{\jmath}\xi)^2 \hat{\varphi}_{k+\frac{1}{2}} = \Delta t (B')^{(n)} 4\pi\kappa(\hat{b}_k - \hat{b}_{k+\frac{1}{2}}),$$

$$-4\pi\kappa\hat{\theta}_{k+\frac{1}{2}} + \left[-\frac{\varepsilon^2}{3(\sigma_s+\kappa)}(\bar{\jmath}\xi)^2 + \kappa\right]\hat{\varphi}_{k+\frac{1}{2}} = 4\pi\kappa(\hat{b}_k - \hat{b}_{k+\frac{1}{2}}),$$

or in matrix notation

$$\text{for } k \geqslant 0: \quad \begin{bmatrix} \varepsilon^2 + C_2\varepsilon^2\xi^2 & \frac{\varepsilon^2\Delta t(B')^{(n)}}{3(\sigma_s+\kappa)}\xi^2 \\ -4\pi\kappa & \kappa + \frac{\varepsilon^2}{3(\sigma_s+\kappa)}\xi^2 \end{bmatrix} \begin{bmatrix} \hat{\theta}_{k+\frac{1}{2}} \\ \hat{\varphi}_{k+\frac{1}{2}} \end{bmatrix} = \begin{bmatrix} C_1 \\ 4\pi\kappa \end{bmatrix} (\hat{b}_k - \hat{b}_{k+\frac{1}{2}}). \tag{3.5}$$

The determinant of the matrix in (3.5) is

$$D = (\varepsilon^2 + C_2\varepsilon^2\xi^2)\left(\kappa + \frac{\varepsilon^2}{3(\sigma_s+\kappa)}\xi^2\right) + \frac{\varepsilon^2\Delta t(B')^{(n)}4\pi\kappa}{3(\sigma_s+\kappa)}\xi^2 = \left(\kappa + \frac{\varepsilon^2}{3(\sigma_s+\kappa)}\xi^2\right)\chi - \kappa C_1 > 0$$

and, therefore, Eq. (3.5) can be explicitly solved for $\hat{\theta}_{k+\frac{1}{2}}$ and $\hat{\varphi}_{k+\frac{1}{2}}$

$$\begin{aligned} \begin{bmatrix} \hat{\theta}_{k+\frac{1}{2}} \\ \hat{\varphi}_{k+\frac{1}{2}} \end{bmatrix} &= \frac{1}{D}\begin{bmatrix} \kappa + \frac{\varepsilon^2}{3(\sigma_s+\kappa)}\xi^2 & -\frac{\varepsilon^2\Delta t(B')^{(n)}}{3(\sigma_s+\kappa)}\xi^2 \\ +4\pi\kappa & \varepsilon^2 + C_2\varepsilon^2\xi^2 \end{bmatrix} \begin{bmatrix} C_1 \\ 4\pi\kappa \end{bmatrix} (\hat{b}_k - \hat{b}_{k+\frac{1}{2}}) = \frac{1}{D}\begin{bmatrix} \kappa C_1 \\ 4\pi\kappa\chi \end{bmatrix}(1-\omega)\hat{b}_k \\ &= \frac{1-\omega}{D}\begin{bmatrix} \kappa C_1 & 0 \\ 4\pi\kappa\chi & 0 \end{bmatrix}\begin{bmatrix} \hat{b}_k \\ \langle \hat{\imath}_k\rangle \end{bmatrix}. \end{aligned} \tag{3.6}$$

Combining (3.3), (3.4) and (3.6), the error of the new scheme after the update is propagated according to

$$\begin{bmatrix} \hat{b}_{k+1} \\ \langle \hat{\imath}_{k+1}\rangle \end{bmatrix} = \begin{bmatrix} \hat{b}_{k+\frac{1}{2}} \\ \langle \hat{\imath}_{k+\frac{1}{2}}\rangle \end{bmatrix} - \begin{bmatrix} \hat{\theta}_{k+\frac{1}{2}} \\ \hat{\varphi}_{k+\frac{1}{2}} \end{bmatrix} = \begin{bmatrix} \omega - \frac{1-\omega}{D}\kappa C_1 & 0 \\ 4\pi\omega_0 - \frac{1-\omega}{D}4\pi\kappa\chi & 0 \end{bmatrix}\begin{bmatrix} \hat{b}_k \\ \langle \hat{\imath}_k\rangle \end{bmatrix}. \tag{3.7}$$

The crucial parameter for convergence is the spectral radius of the matrix on the right side. It is given by

$$\rho \equiv \rho(\varepsilon,\xi) = \left|\omega(\varepsilon,\xi) - \frac{1-\omega(\varepsilon,\xi)}{D(\varepsilon,\xi)}\kappa C_1\right|. \tag{3.8}$$

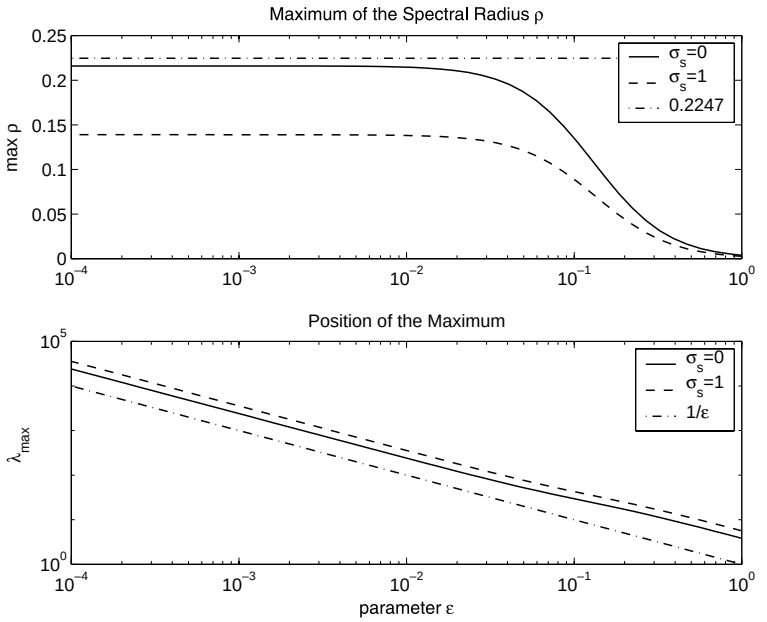

Fig. 2. Value and position of the maximal spectral radius of the preconditioned iteration as a function of the asymptotic parameter ε. For vanishing ε the maximum approaches an upper bound. The position is $O(\varepsilon^{-1})$ for $\varepsilon \to 0$.

It has the properties

- $\rho(\varepsilon, \xi) < \rho_0(\varepsilon, \xi) < 1$, since $0 < \kappa C_1 < D$ and $0 < \omega < 1$,
- $\lim_{(\varepsilon,\xi)\to(0,0)} \rho(\varepsilon, \xi) = 0$,
- $\forall \varepsilon > 0: \quad \lim_{\xi\to\pm\infty} \rho(\varepsilon, \xi) = 0$, and
- $\max_{\xi} \rho(\varepsilon, \xi) \leqslant 0.2247$, for typical cases in glass applications.

Hence, the preconditioned iteration converges faster than the original iteration. In particular, the long-wavelength parts of the error are well damped in contrast to the previous behaviour (Fig. 1). Most important is, however, the fact that the spectral radius has an upper bound significantly less than 1. Therefore, the approach meets the central goal of the preconditioning, as desired. The maximum of the spectral radius ρ as a function of ε was determined numerically. In all of the cases investigated it did not exceed values of approximately 0.2247 (Fig. 2). Numerical evidence suggests, therefore, that the spectral radius of the preconditioned iteration is bounded, although the author does not have a proof for this conjecture. It should be noted that this property is also an important feature of the DSA method for the transport equation. This emphasizes again the analogy between the two preconditioning techniques.

4. Fully discretized RHT system

The fully discretized heat equation using finite differences is given by

$$\varepsilon^2 B_i^{(n+1)} - \Delta t (B')_i^{(n)} (\langle I_{i,\cdot}^{(n+1)} \rangle - 4\pi\kappa B_i^{(n+1)}) - \varepsilon^2 k \Delta t \frac{B_{i+1}^{(n+1)} - 2B_i^{(n+1)} + B_{i+1}^{(n+1)}}{\Delta x^2} = \varepsilon^2 B_i^{(n)}. \tag{4.1a}$$

An equidistant discretization with mesh size Δx is used on the infinite space domain: $x_i = i\Delta x$, $i \in \mathbb{Z}$. For the transport equation we use diamond differenced space discretization together with the discrete ordinates

method for the direction variable μ [11]. The discrete ordinates are given by the knots μ_j of an even order Gauss quadrature rule $\{\mu_j, w_j\}$, $j = 1, \ldots, N$, where w_j are the weights and N is even

$$\varepsilon\mu_j \frac{I^{(n+1)}_{i+1,j} - I^{(n+1)}_{i,j}}{\Delta x} + (\sigma_s + \kappa) I^{(n+1)}_{i+\frac{1}{2},j} - \frac{\sigma_s}{4\pi} \left\langle I^{(n+1)}_{i+\frac{1}{2},\cdot} \right\rangle = \kappa B^{(n+1)}_{i+\frac{1}{2}}. \tag{4.1b}$$

The quantities with index $i+\frac{1}{2}$ are according to diamond differencing defined by cell averages

$$I^{(n+1)}_{i+\frac{1}{2},j} = \frac{I^{(n+1)}_{i+1,j} + I^{(n+1)}_{i,j}}{2}.$$

Solving the coupled system using the Gauss–Seidel method we have the following scheme for $k \geqslant 1$:

$$\varepsilon^2 \overline{B_{i,k+1}} - \Delta t k (\langle \overline{I_{i,k+1}} \rangle - 4\pi\kappa \overline{B_{i,k+1}}) - \varepsilon^2 k \Delta t \frac{B_{i+1,k+1} - 2B_{i,k+1} + B_{i-1,k+1}}{\Delta x^2} = \varepsilon^2 B^{(n)}_i, \tag{4.2a}$$

$$\varepsilon\mu_j \frac{I_{i+1,j,k+1} - I_{i+1,j,k+1}}{\Delta x} + (\sigma_s + \kappa) I_{i+\frac{1}{2},j,k+1} = \frac{\sigma_s}{4\pi} \langle I_{i+\frac{1}{2},\cdot,k+1} \rangle + \kappa B_{i+\frac{1}{2},k}. \tag{4.2b}$$

The bar denotes spatial averaging. Given a vector $q = (q_i)$ of nodal values, the average $\overline{q_i}$ is defined by

$$\overline{q_i} = \frac{q_{i+1} + 2q_i + q_{i-1}}{4}.$$

A Fourier ansatz for the discrete errors

$$b_{i,k} = \hat{b}_k(\xi)\, \mathrm{e}^{\bar{\jmath}\xi x_i}, \quad i_{i,j,k} = \hat{\imath}_{j,k}(\xi)\, \mathrm{e}^{\bar{\jmath}\xi x_i}$$

gives

$$\left[\varepsilon^2 + \Delta t (B')^{(n)}_i 4\pi\kappa\right] \frac{\mathrm{e}^{\bar{\jmath}\xi\Delta x} + 2 + \mathrm{e}^{-\bar{\jmath}\xi\Delta x}}{4} - \varepsilon^2 k \Delta t \frac{\mathrm{e}^{\bar{\jmath}\xi\Delta x} - 2 + \mathrm{e}^{-\bar{\jmath}\xi\Delta x}}{\Delta x^2} \hat{b}_{i,k+1}$$
$$- \Delta t (B')^{(n)}_i \frac{\mathrm{e}^{\bar{\jmath}\xi\Delta x} + 2 + \mathrm{e}^{-\bar{\jmath}\xi\Delta x}}{4} \langle \hat{\imath}_{\cdot,k+1} \rangle = 0,$$

$$\left[\varepsilon\mu_j \frac{\mathrm{e}^{\bar{\jmath}\xi\Delta x} - 1}{\Delta x} + (\sigma_s + \kappa) \frac{\mathrm{e}^{\bar{\jmath}\xi\Delta x} + 1}{2} - \frac{\sigma_s}{4\pi} \frac{\mathrm{e}^{\bar{\jmath}\xi\Delta x} + 1}{2} \langle\cdot\rangle\right] \hat{\imath}_{j,k+1} = \kappa \frac{\mathrm{e}^{\bar{\jmath}\xi\Delta x} + 1}{2} \hat{b}_k,$$

or, using the Euler's representation of the complex exponential function,

$$\left[\varepsilon^2 + \Delta t (B')^{(n)}_i 4\pi\kappa \cos^2\left(\frac{\xi\Delta x}{2}\right) + \varepsilon^2 k \Delta t \frac{4}{\Delta x^2} \sin^2\left(\frac{\xi\Delta x}{2}\right)\right] \hat{b}_{k+1}$$
$$- \Delta t (B')^{(n)}_i 4\pi\kappa \cos^2\left(\frac{\xi\Delta x}{2}\right) \langle \hat{\imath}_{\cdot,k+1} \rangle = 0, \tag{4.3a}$$

$$\left[\varepsilon\mu_j \frac{2\bar{\jmath}}{\Delta x} \sin\left(\frac{\xi\Delta x}{2}\right) + (\sigma_s + \kappa) \cos\left(\frac{\xi\Delta x}{2}\right) - \cos\left(\frac{\xi\Delta x}{2}\right) \frac{\sigma_s}{4\pi} \langle\cdot\rangle\right] \hat{\imath}_{j,k+1} = \kappa \cos\left(\frac{\xi\Delta x}{2}\right) \hat{b}_k. \tag{4.3b}$$

Dividing both equations by the cosine, redefining the constants

$$C_1 = \Delta t (B')^{(n)}_i 4\pi\kappa, \quad C_2 = k\Delta t, \quad \chi = \varepsilon^2 + C_1 + C_2 \varepsilon^2 \Lambda^2$$

in the context of the discretized variables and introducing the new variable

$$\Lambda = \frac{2}{\Delta x}\tan\frac{\xi\Delta x}{2} = \frac{\tan\frac{\xi\Delta x}{2}}{\frac{\xi\Delta x}{2}}\xi$$

for notational convenience, makes it possible to write

$$\hat{b}_{k+1} = \frac{C_1}{\chi}\langle\hat{\imath}_{\cdot,k+1}\rangle,$$

$$\bar{\jmath}\varepsilon\mu_j\Lambda\hat{\imath}_{j,k+1} + (\sigma_s+\kappa)\hat{\imath}_{j,k+1} = \frac{\sigma_s}{4\pi}\langle\hat{\imath}_{\cdot,k+1}\rangle + \kappa\hat{b}_k.$$

As before, the bracket $\langle\hat{\imath}_{\cdot,k+1}\rangle$ can be calculated. In order to do so, the quantity

$$S = \frac{1}{2}\sum_{j=1}^{N}\frac{w_j}{1+\bar{\jmath}\left(\frac{\varepsilon\Lambda\mu_j}{\kappa+\sigma_s}\right)^2} = \frac{1}{2}\sum_{j=1}^{N}\frac{w_j}{1+\left(\frac{\varepsilon\Lambda\mu_j}{\kappa+\sigma_s}\right)^2}$$

is redefined as well. Summing the transport equation over j then yields

$$\langle\hat{\imath}_{\cdot,k+1}\rangle = 2\pi\sum_{j=1}^{N}\hat{\imath}_{j,k+1}w_j = \left(\frac{\sigma_s}{\kappa+\sigma_s}\langle\hat{\imath}_{\cdot,k+1}\rangle + \frac{\kappa}{\kappa+\sigma_s}4\pi\hat{b}_k\right)S.$$

Here, we have to make the assumption that the knots and weights of the quadrature rule $\{\mu_j, w_j\}$ are symmetric and that the number N of knots is even. This is true, in particular, for even order Gauss quadrature. After setting

$$\omega_0 = \frac{\frac{\kappa}{\sigma_s+\kappa}S}{1-\frac{\sigma_s}{\sigma_s+\kappa}S} \quad\text{and}\quad \omega = \frac{C_1}{\chi}\omega_0,$$

the evolution of the Fourier mode ξ may be summarized by the 2×2 system

$$\text{for } k \geqslant 0: \quad \begin{bmatrix}\hat{b}_{k+1}\\ \langle\hat{\imath}_{k+1}\rangle\end{bmatrix} = \begin{bmatrix}\omega & 0\\ 4\pi\omega_0 & 0\end{bmatrix}\begin{bmatrix}\hat{b}_k\\ \langle\hat{\imath}_k\rangle\end{bmatrix}. \tag{4.4}$$

Formally, this is the same result that was obtained above in the case of continuous space and directions. The difference is the factor

$$\frac{\tan\frac{\xi\Delta x}{2}}{\frac{\xi\Delta x}{2}}$$

in the definition of χ and S, respectively. It converges to 1 when ξ tends to zero such that χ and S are reduced to the form they have in the continuous case. But they may differ significantly when ξ is large depending on the value of the grid size Δx. Λ takes the place of ξ. Nevertheless, the spectral radius $\rho_0 = |\omega|$ of the simple Gauss–Seidel iteration retains the relevant properties in the discrete case as before:

$$\rho_0(\varepsilon,\xi) < 1 \quad\text{and}\quad \lim_{\xi\to 0}\rho_0(\varepsilon,\xi) = \frac{C_1}{\varepsilon^2+C_1}, \qquad \lim_{(\varepsilon,\xi)\to(0,0)}\rho_0(\varepsilon,\xi) = 1.$$

The same analysis can be performed for the preconditioned iteration in discretized form. As in Section 3, we start with a step of the simple Gauss–Seidel iteration

$$\varepsilon^2\overline{B_{i,k+\frac{1}{2}}} - \Delta t(B')_i^{(n)}(\langle\overline{I_{i,k+\frac{1}{2}}}\rangle - 4\pi\kappa\overline{B_{i,k+\frac{1}{2}}}) - \varepsilon^2 k\Delta t\frac{B_{i+1,k+\frac{1}{2}} - 2B_{i,k+\frac{1}{2}} + B_{i-1,k+\frac{1}{2}}}{\Delta x^2} = \varepsilon^2 B_i^{(n)}, \tag{4.5a}$$

$$\varepsilon\mu_j\frac{I^{(n+1)}_{i+\frac{1}{2},j,k+1} - I^{(n+1)}_{i+1,j,k+\frac{1}{2}}}{\Delta x} + (\sigma_s+\kappa)I^{(n+1)}_{i+\frac{1}{2},j,k+\frac{1}{2}} = \frac{\sigma_s}{4\pi}\left\langle I^{(n+1)}_{i+\frac{1}{2},\cdot,k+\frac{1}{2}}\right\rangle + \kappa B^{(n+1)}_{i+\frac{1}{2},k}. \tag{4.5b}$$

Next, the P_1 discretization in the following discretized form is solved:

$$\varepsilon^2\overline{\theta_{i,k+\frac{1}{2}}} - \varepsilon^2 C_2\frac{\theta_{i+1,k+\frac{1}{2}} - 2\theta_{i,k+\frac{1}{2}} + \theta_{i-1,k+\frac{1}{2}}}{\Delta x^2} - \frac{\varepsilon^2\Delta t(B')_i^{(n)}}{3(\kappa+\sigma_s)}\frac{\varphi_{i+1,k+\frac{1}{2}} - 2\varphi_{i,k+\frac{1}{2}} + \varphi_{i-1,k+\frac{1}{2}}}{\Delta x^2}$$
$$= \Delta t(B')_i^{(n)}4\pi\kappa(\overline{B_{i,k+\frac{1}{2}}} - \overline{B_{i,k}}),$$

$$-\frac{\varepsilon^2}{3(\kappa+\sigma_s)}\frac{\varphi_{i+1,k+\frac{1}{2}} - 2\varphi_{i,k+\frac{1}{2}} + \varphi_{i-1,k+\frac{1}{2}}}{\Delta x^2} + \kappa\overline{\varphi_{i,k+\frac{1}{2}}} = 4\pi\kappa\overline{\theta_{i,k+\frac{1}{2}}} + 4\pi\kappa(\overline{B_{i,k+\frac{1}{2}}} - \overline{B_{i,k}})$$

and, finally, an update is made

$$B_{i,k+1} = B_{i,k+\frac{1}{2}} + \theta_{i,k+\frac{1}{2}},$$

$$\langle I_{i,\cdot,k+1}\rangle = \langle I_{i,\cdot,k+\frac{1}{2}}\rangle + \varphi_{i,k+\frac{1}{2}}.$$

Introducing the Fourier ansatz for the errors, we have in the first substep

$$\text{for } k \geqslant 0: \quad \begin{bmatrix}\hat{b}_{k+\frac{1}{2}}\\ \langle\hat{\imath}_{k+\frac{1}{2}}\rangle\end{bmatrix} = \begin{bmatrix}\omega & 0\\ 4\pi\omega_0 & 0\end{bmatrix}\begin{bmatrix}\hat{b}_k\\ \langle\hat{\imath}_k\rangle\end{bmatrix}, \tag{4.6}$$

as previously shown for the Gauss–Seidel iteration. Moreover, after some manipulations the P_1 system gives

$$\left(\varepsilon^2 + \varepsilon^2 C_2\Lambda^2\right)\hat{\theta}_{k+\frac{1}{2}} - \frac{\varepsilon^2\Delta t(B')^{(n)}}{3(\sigma_s+\kappa)}\Lambda^2 = C_1(\hat{b}_k - \hat{b}_{k+\frac{1}{2}}),$$

$$-4\pi\kappa\hat{\theta}_{k+\frac{1}{2}} + \left(\frac{\varepsilon^2}{3(\sigma_s+\kappa)}\Lambda^2 + \kappa\right)\hat{\varphi}_{k+\frac{1}{2}} = 4\pi\kappa(\hat{b}_k - \hat{b}_{k+\frac{1}{2}}),$$

or in matrix notation ($k \geqslant 0$):

$$\begin{bmatrix}\varepsilon^2 + C_2\varepsilon^2\Lambda^2 & \frac{\varepsilon^2\Delta t(B')^{(n)}}{3(\sigma_s+\kappa)}\Lambda^2\\ -4\pi\kappa & \kappa + \frac{\varepsilon^2}{3(\sigma_s+\kappa)}\Lambda^2\end{bmatrix}\begin{bmatrix}\hat{\theta}_{k+\frac{1}{2}}\\ \hat{\varphi}_{k+\frac{1}{2}}\end{bmatrix} = \begin{bmatrix}C_1\\ 4\pi\kappa\end{bmatrix}(\hat{b}_k - \hat{b}_{k+\frac{1}{2}}).$$

The corresponding determinant is

$$D = \left(\varepsilon^2 + C_2\varepsilon^2\Lambda^2\right)\left(\kappa + \frac{\varepsilon^2}{3(\sigma_s+\kappa)}\Lambda^2\right) + \frac{\varepsilon^2 C_1}{3(\sigma_s+\kappa)}\Lambda^2 = \left(\kappa + \frac{\varepsilon^2}{3(\sigma_s+\kappa)}\Lambda^2\right)\chi - \kappa C_1 > 0$$

and the matrix can be inverted. This yields

$$\begin{bmatrix} \hat{\theta}_{k+\frac{1}{2}} \\ \hat{\varphi}_{k+\frac{1}{2}} \end{bmatrix} = \frac{1}{D} \begin{bmatrix} \kappa + \frac{\varepsilon^2}{3(\sigma_s+\kappa)} \Lambda^2 & -\frac{\varepsilon^2 \Delta t (B')^{(n)}}{3(\sigma_s+\kappa)} \Lambda^2 \\ +4\pi\kappa & \varepsilon^2 + C_2 \varepsilon^2 \Lambda^2 \end{bmatrix} \begin{bmatrix} C_1 \\ 4\pi\kappa \end{bmatrix} (\hat{b}_{k+\frac{1}{2}} - \hat{b}_k)$$

$$= \frac{1}{D} \begin{bmatrix} \kappa C_1 \\ 4\pi\kappa\chi \end{bmatrix} (\omega - 1)\hat{b}_k = \frac{\omega - 1}{D} \begin{bmatrix} \kappa C_1 & 0 \\ 4\pi\kappa\chi & 0 \end{bmatrix} \begin{bmatrix} \hat{b}_k \\ \langle \hat{i}_k \rangle \end{bmatrix}. \tag{4.7}$$

Putting Eqs. (4.6) and (4.7) together yields

$$\begin{bmatrix} \hat{b}_{k+1} \\ \langle \hat{i}_{k+1} \rangle \end{bmatrix} = \begin{bmatrix} \omega - \frac{1-\omega}{D} \kappa C_1 & 0 \\ 4\pi\omega_0 - \frac{1-\omega}{D} 4\pi\kappa\chi & 0 \end{bmatrix} \begin{bmatrix} \hat{b}_k \\ \langle \hat{i}_k \rangle \end{bmatrix} \tag{4.8}$$

and the spectral radius has again the form

$$\rho \equiv \rho(\varepsilon, \Lambda) = \left| \omega(\varepsilon, \Lambda) - \frac{1 - \omega(\varepsilon, \Lambda)}{D(\varepsilon, \Lambda)} \kappa C_1 \right|.$$

Furthermore, the properties of ρ remain unchanged, namely,

- $\rho(\varepsilon, \Lambda) < \rho_0(\varepsilon, \Lambda) < 1$, since $0 < \kappa C_1 < D$ and $0 < \omega < 1$,
- $\lim_{(\varepsilon,\Lambda)\to(0,0)} \rho(\varepsilon, \Lambda) = 0$,
- $\forall \varepsilon > 0: \quad \lim_{\Lambda \to \pm\infty} \rho(\varepsilon, \Lambda) = 0$, and
- $\max_{\Lambda} \rho(\varepsilon, \Lambda) \leqslant 0.2247$.

It should be mentioned that this result ows to the consistent discretization of the original system and its P_1 approximation. If diamond differencing is used for the transport equation then the corresponding P_1 approximation must be discretized using three point averages. This has been observed in the realm of transport theory and has been a major contribution to the success of the DSA algorithm [2,11,12]. In the present case, these findings imply, moreover, that also the heat equation has to include similar averages such that the terms in (4.8) are correctly balanced. Other discretizations for the transport equation may be used, of course, and in these cases different consistent discretizations will have to be derived.

It is known in the literature that the discretization of the transport equation using diamond differencing (DD) can lead to numerical problems if the regime is optically thick [1]. Unphysical oscillations are observed in the numerical solution for the radiative intensity. The use of the consistent discretization of the RHT equations introduces averages of I and B in the temperature equation to make the accelerated method convergent. This smoothes the oscillations of I in the temperature equation and stabilizes the discretization. Unphysical numerical results, e.g., oscillations owing to problems with DD, have not been observed for the temperature in our numerical experiments.

5. Numerical comparisons

As a test example we considered a RHT problem in the form

$$\varepsilon^2 \frac{\partial T}{\partial t} = \varepsilon^2 \partial_x (k \partial_x T) + \langle \kappa (I - B) \rangle, \tag{5.1a}$$

$$\forall \mu \in [-1, 1]: \quad \varepsilon \mu \partial_x I + \sigma_s I = \frac{1}{4\pi} \langle \sigma_s I \rangle + \kappa (B - I), \tag{5.1b}$$

$$\forall \mu > 0: \quad I(\mu, 0) = I_b(\mu, 0) \quad \text{and} \quad \forall \mu < 0: \quad I(\mu, 1) = I_b(\mu, 1) \tag{5.1c}$$

with Dirichlet boundary conditions for the temperature

$$T(0) = T_l, \quad T(1) = T_r. \tag{5.1d}$$

The heat conductivity in the heat equation for the temperature was $k = 1$. We considered the radiative transport equation with pure absorption and no scattering $\kappa = 1$, $\sigma = 0$ as is frequently done in models for hot glass or for gas in the combustion chamber of turbines. The initial value for the temperature at the beginning was the sine-shaped profile $T_0(x) = 1000 + 100\sin(\pi x)$. The boundary values T_l and T_r had the same value 1000 K. To these temperatures correspond the boundary values for the radiative intensity I which were given by Stefan's Law for air outside of the domain $I_b = B^a(T_b) = n_a^2 \frac{\sigma}{\pi} T_b^4$. The refractive indices were $n = 1.46$ for glass and $n_a = 1.00$ for air, respectively. We discretized the equation using an equidistant mesh in space and in time. A stepsize of $\Delta t = 10^{-6}$ for the time and 129 spatial knots corresponding to $\Delta x = 2^{-7}$ were used. The evolution was computed until the final time $t = 10^{-3}$.

Fig. 3 shows a comparison of the error reduction rates obtained for the simple iteration without preconditioning and for the accelerated iteration with preconditioning. The ratio of the residual of two successive iterates r_k/r_{k-1} was monitored during the first time step Δt (convergence was the same for other time steps). For vanishing ε, the former approaches 1 while the latter remains bounded away from 1, as expected.

Table 1 displays the runtimes for solving the RHT problem. The data were measured on a Pentium 4 (1 GHz) running MATLAB 5 under Linux kernel 2.4.16. We compared the runtimes of the preconditioned block Gauss–Seidel method presented in this paper with the simple block Gauss–Seidel iteration and various other solvers. These other solvers are based on a formulation of the time discretized equations in terms of a nonlinear stationary RHT problem at each time step. Firstly, Newton's method was applied to the nonlinear equation for T that had to be solved at each time step. Secondly, the multilevel approaches proposed in [5] were implemented. The nested Newton's method computes the solution of the RHT equations on a coarse level using Newton's method and takes this solution as the initial iterate on the

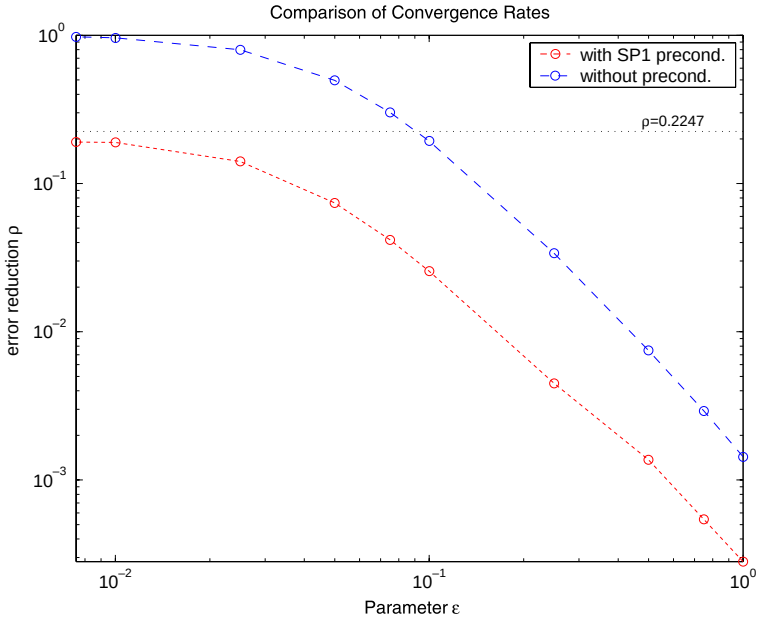

Fig. 3. Error reduction rates of the simple Gauss–Seidel iteration and the preconditioned iteration. The first time-step of the evolution of the RHT problem with Dirichlet boundary conditions for the temperature was examined by monitoring the relative residuals r_k/r_{k-1}.

Table 1
Run times (seconds) for solving the RHT system using different mesh sizes

n_x	GS	PGS	N	nN	nAB	nK
33	0.05	0.06	0.10	0.09	0.10	0.09
65	0.09	0.11	0.16	0.14	0.17	0.14
129	0.17	0.20	0.29	0.24	0.30	0.24
257	0.36	0.60	0.63	0.46	0.54	0.42
513	0.81	1.68	1.38	0.94	1.04	0.76
1025	2.29	5.49	3.30	2.05	2.17	1.52

The solvers compared are Gauss–Seidel (GS), preconditioned Gauss–Seidel (PGS), Newton's method (N), a nested Newton (nN), nested Atkinson–Brakhage (nAB) and Kelley's nested norm-convergent method (nK). The parameter value was $\varepsilon = 1$.

subsequent fine mesh level, and proceeds in this way from the coarsest to the finest mesh. The nested Atkinson–Brakhage method and Kelley's nested norm-convergent variant of the Atkinson–Brakhage solver also rely on this cascading of the initial iterates from coarse to fine meshes but they use different solvers instead of Newton's method at each level. In [5] it has been shown that Kelley's method performs best among these multilevel solvers and it should, therefore, also perform better than Newton's method. We compare our linear scheme, which relies on a preconditioner that is specifically adapted to the equation, with these efficient nonlinear solvers for the RHT equation.

We solved the discretized system using different mesh sizes in order to assess how the preconditioned iteration performs compared with, in particular, the fast multilevel solvers. As can be seen in Table 1, the simple block iteration is – in the case $\varepsilon = 1$ – faster than the preconditioned iteration owing to the fact that only few iterations were needed for convergence and the additional cost of the preconditioner was significant, in particular when the system was large. Newton's iteration was more time-consuming than the preconditioned scheme while the three multilevel approaches were faster when the system became large, i.e., for $n_x \geqslant 257$. This is what we would expect when using multilevel methods. In particular, Kelley's solver outperforms all of the other solvers in this case. Although the preconditioned scheme was sufficiently fast for the small- to moderate-sized meshes it's timing result was poor for the large mesh with $n_x = 1025$.

Finally, the runtimes in Table 2 show how the solvers perform when the regime becomes optically thick for small values of ε. The runtimes for the simple Gauss–Seidel iteration without preconditioning increased tremendously when ε approached the value 0.01 and convergence could hardly be achieved. Interestingly, also Newtons method and nested Newton's method suffered from slower convergence in the optically thick case. In contrast, the preconditioned iteration remained remarkably unaffected from the strong optical thickness as can be observed from the moderate increase of the runtimes.

Table 2
Run times (seconds) for solving the RHT system with variable parameter ε (mesh size $\Delta x = 2^{-7}$)

ε	GS	PGS	N	nN
1	0.17	0.20	0.29	0.24
0.75	0.18	0.23	0.31	0.25
0.5	0.23	0.26	0.41	0.26
0.25	0.33	0.31	0.55	0.29
0.1	1.02	0.40	1.04	0.60
0.075	1.62	0.43	1.14	0.76
0.05	3.28	0.47	1.59	0.90
0.025	11.26	0.48	2.62	1.21
0.01	64.93	0.49	6.62	2.99

6. Conclusions

In this paper, we have presented a new solver for the fast solution of the radiative heat transfer equations, i.e., a coupled system of a heat equation and a transport equation. We proposed a particular preconditioner that is adapted to the RHT problem in the optically thick regime. It is based on the P_1 approximation to the radiative heat transfer equations and extends the ideas underlying the DSA algorithm for the stationary transport equation. In [10] it has been shown that the P_1 equations are a good approximation to the RHT equations for glass and that they perform particularly well in the optically thick case.

We performed a von Neumann analysis to study the convergence properties of the simple and the preconditioned block Gauss–Seidel iterations. This analysis showed that the use of the P_1 approximation as a preconditioner can successfully improve on the simple iteration by improving the error reduction of the long-wavelength parts of the error.

Numerical experiments confirmed these findings and showed that the preconditioned iteration performs much better in the optically thick regime than the simple iteration. Nevertheless, the higher cost for preconditioning must be kept in mind. It should be noted, moreover, that the preconditioned iteration is also faster than nested Newton's method when ε becomes small. This sophisticated method based on a multilevel approach is known to be very efficient in solving RHT problems.

The method we propose uses DSA for solving the radiative transport equation. Original DSA is restricted to one space dimension and the present study is concerned only with this case. Recent results indicate, however, that DSA can be extended to higher dimensions [4,6]. Hence, the method should be feasible in multi-dimensional geometries as well. Furthermore, for the sake of simplicity, the presentation focuses on the frequency independent, grey model, but the results can be transferred to more general cases as well. The same remark applies to the transparent boundary conditions for the transfer equation, where general semi-transparent boundary conditions can be dealt with in a similar way.

Acknowledgements

The author thanks Axel Klar for many helpful discussions during the writing of this paper. This work was supported by DFG Grant KL 1105/7 and by SFB 568.

Appendix A. Gauss–Seidel iteration (II)

When the lower triangular matrix is used in (2.2c) the linear iteration is given by

$$\text{for } k \geqslant 0: \quad \begin{bmatrix} A_{11} & 0 \\ A_{21} & A_{22} \end{bmatrix} \begin{bmatrix} B_{k+1} \\ I_{k+1} \end{bmatrix} = \begin{bmatrix} \varepsilon^2 B^{(n)} - A_{12} I_k \\ 0 \end{bmatrix}$$

and the corresponding system for the errors is then

$$\text{for } k \geqslant 0: \quad \begin{bmatrix} A_{11} & 0 \\ A_{21} & A_{22} \end{bmatrix} \begin{bmatrix} b_{k+1} \\ i_{k+1} \end{bmatrix} = \begin{bmatrix} -A_{12} i_k \\ 0 \end{bmatrix}$$

or more explicitly

$$\left[\varepsilon^2 + \Delta t (B')^{(n)} 4\pi\kappa - \varepsilon^2 \Delta t (B')^{(n)} \partial_x \left(\frac{k}{(B')^{(n)}} \partial_x (\cdot) \right) \right] b_{k+1} = \Delta t (B')^{(n)} \langle i_k \rangle,$$

$$\left[\varepsilon\mu\partial(\cdot)+\sigma_s+\kappa-\frac{\sigma_s}{4\pi}\langle\cdot\rangle\right]i_{k+1}=\kappa b_{k+1}.$$

The Fourier ansatz for the errors b_{k+1} and i_{k+1} leads to

$$\left[\varepsilon^2+\Delta t(B')^{(n)}4\pi\kappa-\varepsilon^2\Delta t(B')^{(n)}(\bar{\jmath}\xi)^2\right]\hat{b}_{k+1}=\Delta t(B')^{(n)}\langle\hat{\imath}_k\rangle,$$

$$\left[\varepsilon\mu(\bar{\jmath}\xi)+\sigma_s+\kappa-\frac{\sigma_s}{4\pi}\langle\cdot\rangle\right]\hat{\imath}_{k+1}=\kappa\hat{b}_{k+1}.$$

Hence, we have

$$\hat{b}_{k+1}=\frac{C_1}{\chi}\langle\hat{\imath}_k\rangle$$

and the bracket $\langle\hat{\imath}_{k+1}\rangle$ is evaluated according to

$$\langle\hat{\imath}_{k+1}\rangle=4\pi\omega_0\hat{b}_{k+1}=\frac{C_1}{\chi}\omega_0\langle\hat{\imath}_k\rangle=\omega\langle\hat{\imath}_k\rangle.$$

The result may be rewritten as a system in the form

$$\text{for } k\geqslant 0: \quad \begin{bmatrix}\hat{b}_{k+1}\\ \langle\hat{\imath}_{k+1}\rangle\end{bmatrix}=\begin{bmatrix}0 & \frac{C_1}{4\pi\chi}\\ 0 & \omega\end{bmatrix}\begin{bmatrix}\hat{b}_k\\ \langle\hat{\imath}_k\rangle\end{bmatrix}. \tag{A.1}$$

The iteration is accelerated by approximating the error equation by the following P_1 system:

$$\left[\varepsilon^2-\varepsilon^2\Delta t(B')^{(n)}\partial_x\left(\frac{k}{(B')^{(n)}}\partial_x(\cdot)\right)\right]\theta_{k+\frac{1}{2}}-\frac{\varepsilon^2\Delta t(B')^{(n)}}{3(\sigma_s+\kappa)}\Delta\varphi_{k+\frac{1}{2}}=\frac{C_1}{4\pi}(\langle i_{k+\frac{1}{2}}\rangle-\langle i_k\rangle),$$

$$\left[-\frac{\varepsilon^2}{3(\sigma_s+\kappa)}\partial_x^2(\cdot)+\kappa\right]\varphi_{k+\frac{1}{2}}=4\pi\kappa\theta_{k+\frac{1}{2}}.$$

Introducing the Fourier ansatz here gives

$$\text{for } k\geqslant 0: \quad \begin{bmatrix}\varepsilon^2+C_2\varepsilon^2\xi^2 & \frac{\varepsilon^2\Delta t(B')^{(n)}}{3(\sigma_s+\kappa)}\xi^2\\ -4\pi\kappa & \kappa+\frac{\varepsilon^2}{3(\sigma_s+\kappa)}\xi^2\end{bmatrix}\begin{bmatrix}\hat{\theta}_{k+\frac{1}{2}}\\ \hat{\varphi}_{k+\frac{1}{2}}\end{bmatrix}=\begin{bmatrix}\frac{C_1}{4\pi}\\ 0\end{bmatrix}(\langle i_{k+\frac{1}{2}}\rangle-\langle i_k\rangle)$$

which upon inversion of the left hand matrix results in

$$\begin{bmatrix}\hat{\theta}_{k+\frac{1}{2}}\\ \hat{\varphi}_{k+\frac{1}{2}}\end{bmatrix}=\frac{\omega-1}{D}\begin{bmatrix}0 & \frac{C_1}{4\pi}\left(\kappa+\frac{\varepsilon^2\xi^2}{3(\kappa+\sigma_s)}\right)\\ 0 & 4\pi\kappa C_1\end{bmatrix}\begin{bmatrix}\hat{b}_k\\ \langle\hat{\imath}_k\rangle\end{bmatrix}.$$

Therefore, the overall matrix for the evolution is

$$\begin{bmatrix}\hat{\theta}_{k+\frac{1}{2}}\\ \hat{\varphi}_{k+\frac{1}{2}}\end{bmatrix}=\begin{bmatrix}0 & \frac{C_1}{4\pi\chi}-\frac{1-\omega}{D}\frac{C_1}{4\pi}\left(\kappa+\frac{\varepsilon^2\xi^2}{3(\kappa+\sigma_s)}\right)\\ 0 & \omega-\frac{1-\omega}{D}\kappa C_1\end{bmatrix}\begin{bmatrix}\hat{b}_k\\ \langle\hat{\imath}_k\rangle\end{bmatrix} \tag{A.2}$$

and the spectral radius, again, takes the form

$$\rho(\varepsilon,\xi)=\left|\ \omega(\varepsilon,\xi)-\frac{1-\omega(\varepsilon,\xi)}{D(\varepsilon,\xi)}\kappa C_1\right|, \tag{A.3}$$

as in Section 3.

Appendix B. Jacobi iteration

Formally, we have the iteration

$$\text{for } k\geqslant 0: \quad \begin{bmatrix} A_{11} & 0\\ 0 & A_{22}\end{bmatrix}\begin{bmatrix} B_{k+1}\\ I_{k+1}\end{bmatrix}=\begin{bmatrix} \varepsilon^2 B^{(n)}-A_{12}I_k\\ -A_{21}B_k\end{bmatrix}.$$

Consequently, the errors fulfill

$$\text{for } k\geqslant 0: \quad \begin{bmatrix} A_{11} & 0\\ 0 & A_{22}\end{bmatrix}\begin{bmatrix} b_{k+1}\\ i_{k+1}\end{bmatrix}=\begin{bmatrix} -A_{12}i_k\\ -A_{21}b_k\end{bmatrix},$$

or more explicitly

$$\left[\varepsilon^2+\Delta t(B')^{(n)}4\pi\kappa-\varepsilon^2\Delta t(B')^{(n)}\partial_x\left(\frac{k}{(B')^{(n)}}\partial_x(\cdot)\right)\right]b_{k+1}=\Delta t(B')^{(n)}\langle i_k\rangle,$$

$$\left[\varepsilon\mu\partial(\cdot)+\sigma_s+\kappa-\frac{\sigma_s}{4\pi}\langle\cdot\rangle\right]i_{k+1}=\kappa b_k.$$

When we introduce the Fourier ansatz we obtain

$$\left[\varepsilon^2+\Delta t(B')^{(n)}4\pi\kappa-\varepsilon^2\Delta t(B')^{(n)}(\bar{\jmath}\xi)^2\right]\hat{b}_{k+1}=\Delta t(B')^{(n)}\langle\hat{\imath}_k\rangle$$

$$\left[\varepsilon\mu(\bar{\jmath}\xi)+\sigma_s+\kappa-\frac{\sigma_s}{4\pi}\langle\cdot\rangle\right]\hat{\imath}_{k+1}=\kappa\hat{b}_k,$$

which can be simplified as before such that we end up with the evolution

$$\text{for } k\geqslant 0: \quad \begin{bmatrix}\hat{b}_{k+1}\\ \langle\hat{\imath}_{k+1}\rangle\end{bmatrix}=\begin{bmatrix} 0 & \frac{C_1}{4\pi\chi}\\ 4\pi\omega_0 & 0\end{bmatrix}\begin{bmatrix}\hat{b}_k\\ \langle\hat{\imath}_k\rangle\end{bmatrix}. \tag{B.1}$$

Therefore, the spectral radius is different, namely is the square root

$$\rho_0(\varepsilon,\xi)=\sqrt{\frac{C_1}{\chi}\omega_0}=\sqrt{\omega}. \tag{B.2}$$

In order to accelerate this Jacobi-type scheme we approximate the error equation by the P_1 system

$$\left[\varepsilon^2-\varepsilon^2\Delta t(B')^{(n)}\partial_x\left(\frac{k}{(B')^{(n)}}\partial_x(\cdot)\right)\right]\theta_{k+\frac{1}{2}}-\frac{\varepsilon^2\Delta t(B')^{(n)}}{3(\sigma_s+\kappa)}\Delta\varphi_{k+\frac{1}{2}}=C_1(B_{k+\frac{1}{2}}-B_k)+\frac{C_1}{4\pi}(\langle I_{k+\frac{1}{2}}\rangle-\langle I_k\rangle),$$

$$-4\pi\kappa\theta_{k+\frac{1}{2}}+\left[-\frac{\varepsilon^2}{3(\sigma_s+\kappa)}\partial_x^2(\cdot)+\kappa\right]\varphi_{k+\frac{1}{2}}=+4\pi\kappa(B_{k+\frac{1}{2}}-B_k),$$

which gives the following equations for the Fourier modes

$$\begin{bmatrix} \varepsilon^2 + C_2\varepsilon^2\xi^2 & \frac{\varepsilon^2\Delta t(B')^{(n)}}{3(\sigma_s+\kappa)}\xi^2 \\ -4\pi\kappa & \kappa + \frac{\varepsilon^2}{3(\sigma_s+\kappa)}\xi^2 \end{bmatrix} \begin{bmatrix} \hat{\theta}_{k+\frac{1}{2}} \\ \hat{\varphi}_{k+\frac{1}{2}} \end{bmatrix} = \begin{bmatrix} C_1 & \frac{C_1}{4\pi} \\ 4\pi\kappa & 0 \end{bmatrix} \begin{bmatrix} \hat{b}_k - \hat{b}_{k+\frac{1}{2}} \\ \langle\hat{\imath}_k\rangle - \langle\hat{\imath}_{k+\frac{1}{2}}\rangle \end{bmatrix}.$$

Inverting the matrix on left and taking (B.1) into account we find

$$\begin{aligned} \begin{bmatrix} \hat{\theta}_{k+\frac{1}{2}} \\ \hat{\varphi}_{k+\frac{1}{2}} \end{bmatrix} &= \frac{1}{D} \begin{bmatrix} \kappa + \frac{\varepsilon^2}{3(\sigma_s+\kappa)}\xi^2 & -\frac{\varepsilon^2\Delta t(B')^{(n)}}{3(\sigma_s+\kappa)}\xi^2 \\ +4\pi\kappa & \varepsilon^2 + C_2\varepsilon^2\xi^2 \end{bmatrix} \begin{bmatrix} C_1 & \frac{C_1}{4\pi} \\ 4\pi\kappa & 0 \end{bmatrix} \cdot \begin{bmatrix} 1 & -\frac{C_1}{4\pi\chi} \\ -4\pi\omega_0 & 1 \end{bmatrix} \begin{bmatrix} \hat{b}_k \\ \langle\hat{\imath}_k\rangle \end{bmatrix} \\ &= \frac{1}{D} \begin{bmatrix} \kappa C_1 - \omega C_1\left(\kappa + \frac{\varepsilon^2\xi^2}{3(\kappa+\sigma_s)}\right) & -\frac{C_1}{4\pi\chi}D \\ 4\pi\kappa(\chi - \omega_0 C_1) & 0 \end{bmatrix} \begin{bmatrix} \hat{b}_k \\ \langle\hat{\imath}_k\rangle \end{bmatrix} \end{aligned}$$

and, hence, the evolution of the accelerated scheme is described by

$$\begin{bmatrix} \hat{b}_{k+1} \\ \langle\hat{\imath}_{k+1}\rangle \end{bmatrix} = \begin{bmatrix} \hat{b}_{k+\frac{1}{2}} \\ \langle\hat{\imath}_{k+\frac{1}{2}}\rangle \end{bmatrix} - \begin{bmatrix} \hat{\theta}_{k+\frac{1}{2}} \\ \hat{\varphi}_{k+\frac{1}{2}} \end{bmatrix} = \frac{1}{D} \begin{bmatrix} \omega_0\frac{C_1}{D}\left(\kappa + \frac{\varepsilon^2\xi^2}{3(\kappa+\sigma_s)}\right) - \frac{1-\omega_0}{D}\kappa C_1 & 0 \\ -4\pi\kappa(\chi - \omega_0 C_1) + 4\pi\omega_0 D & 0 \end{bmatrix} \begin{bmatrix} \hat{b}_k \\ \langle\hat{\imath}_k\rangle \end{bmatrix}. \tag{B.3}$$

Eventually, the spectral radius is found to be given by

$$\rho = \omega_0\frac{C_1}{D}\left(\kappa + \frac{\varepsilon^2\xi^2}{3(\kappa+\sigma_s)}\right) - \frac{1-\omega_0}{D}\kappa C_1. \tag{B.4}$$

References

[1] Marwin L. Adams, Edward W. Larsen, Fast iterative methods for discrete-ordinates particle transport computations, Prog. Nucl. Energy 40 (1) (2001) 3–159.

[2] R.E. Alcouffe, Diffusion synthetic acceleration methods for the diamond-differenced discrete-ordinates equations, Nucl. Sci. Eng. 64 (1977) 344–355.

[3] R.E. Alcouffe, Bradley A. Clark, Edward W. Larsen, The diffusion-synthetic acceleration of transport iterations with application to a radiation hydrodynamics problem, in: Multiple Time Scales.

[4] S.F. Ashby, P.N. Brown, M.R. Dorr, A.C. Hindmarsh, A linear algebraic analysis of diffusion synthetic acceleration for the Boltzmann transport equation, SIAM J. Num. Anal. 32 (1) (1995) 128–178.

[5] J.M. Banoczi, C.T. Kelley, A fast multilevel algorithm for the solution of nonlinear systems of conductive–radiative heat transfer equations, SIAM J. Sci. Comp. 19 (1) (1998) 266–279.

[6] Peter N. Brown, A linear algebraic development of diffusion synthetic acceleration for three-dimensional transport equations, SIAM J. Num. Anal. 32 (1) (1995) 179–214.

[7] J.A. Fleck Jr., J.D. Cummings, An implicit Monte Carlo scheme for calculating time and frequency dependent nonlinear radiation transport, J. Comp. Phys. 8 (1971) 313–342.

[8] Robert Howell, John R. Siegel, Thermal Radiation Heat Transfer, third ed., Taylor & Francis, London, 1992.

[9] E.W. Larsen, Diffusion theory as an asymptotic limit of transport theory for nearly critical systems with small mean free paths, Ann. Nucl. Energy 7 (1980) 249.

[10] E.W. Larsen, G. Thömmes, A. Klar, M. Seaïd, T. Götz, Simplified P_N approximations to the equations of radiative heat transfer and applications, J. Comp. Phys. 183 (2002) 652–675.

[11] Edward W. Larsen, Unconditionally stable diffusion-synthetic acceleration methods for the slab geometry discrete ordinates equations. Part I: theory, Nucl. Sci. Eng. 82 (1982) 47–63.

[12] Edward W. Larsen, Diffusion-synthetic acceleration methods for discrete-ordinate problems, Transp. Theory Statist. Phys. 13 (182) (1984) 107–126.

[13] Edward W. Larsen, J.E. Morel, John M. McGhee, Asymptotic derivation of the multigroup P_1 and simplified P_N equations with anisotropic scattering, Nucl. Sci. Eng. 12 (1996) 328–342.

[14] M.F. Modest, Radiative Heat Transfer, McGraw-Hill, New York, 1993.

[15] J.E. Morel, Todd A. Wareing, Kenneth Smith, A linear-discontinuous spatial differencing scheme for s_n radiative transfer calculations, J. Comp. Phys. 128 (1996) 445–462.
[16] G.C. Pomraning, Asymptotic and variational derivations of the simplified P_n equations, Ann. Nucl. Energy 20 (1993) 623.
[17] Djordje I. Tomašević, Edward W. Larsen, The simplified P_2 approximation, Nucl. Sci. Eng. 122 (1996) 309–325.
[18] R. Viskanta, E.E. Anderson, Heat transfer in semitransparent solids, Adv. Heat Transf. 11 (1975) 318.
[19] Raymond. Viskanta, Radiative heat transfer, Fortschritte der Verfahrenstechnik 22 (1984) 51–81.